Passive SAR imaging using a satellite pulsed radar as an illuminator of opportunity

P. Samczynski, K. Kulpa
Institute of Electronic Systems
Warsaw University of Technology
Warszawa, Poland
psamczyn@elka.pw.edu.pl

Abstract—**This paper presents the analysis and simulation results of a ground stationary passive synthetic aperture radar (SAR) receiver using a spaceborne SAR as an illuminator. In the paper, the bistatic geometry of passive SAR is presented and the expected resolutions are discussed and compared to the monostatic case. Finally, the results of the signal processing for both active and passive SAR imaging are presented. The main goal of the analysis performed was to develop and test new passive SAR algorithms dedicated for the passive SAR receiver developed at the Warsaw University of Technology. The results obtained verify the feasibility of the proposed passive SAR imaging algorithm.**

Keywords-passive SAR, bistatic SAR, PCL, GSM passive radar, air survaillance

I. INTRODUCTION

Over recent years a few bistatic radar experiments have been carried out using ground stationary receivers and spaceborne illuminators [1], [5], [6], [8]. Most of them were conducted successfully and the results show new capabilities of SAR imaging [1], [5], [6], [8]. Taking into account the advantage of the use of bistatic geometry [1], [2] and its low cost nature, passive SAR technology seems to be a good candidate as an additional sensor in the future in regards to Earth monitoring.

Recently, the Warsaw University of Technology started research in passive SAR. The first step was designing the passive radar receiver and recording the real signal using the EnviSat-1 satellite as an illuminator [9]. The first raw radar data was successfully collected during trials carried out in 2011 [9]. The second and parallel step was to develop passive SAR algorithms and test them using simulated data generated by the Raw Radar Simulator [10]. The results of this stage of research are presented in this paper.

II. PASSIVE SAR BISTATIC GEOMETRY

The simplified bistatic radar geometry for a stationary ground receiver has been presented in Fig. 1. The illuminator of opportunity is a SAR radar mounted to the spaceborne platform flying with the constant velocity v at the altitude H above the ground level. The distance between the radar transmitter (Tx) and passive receiver (Rx) equals $R_T(t)$.

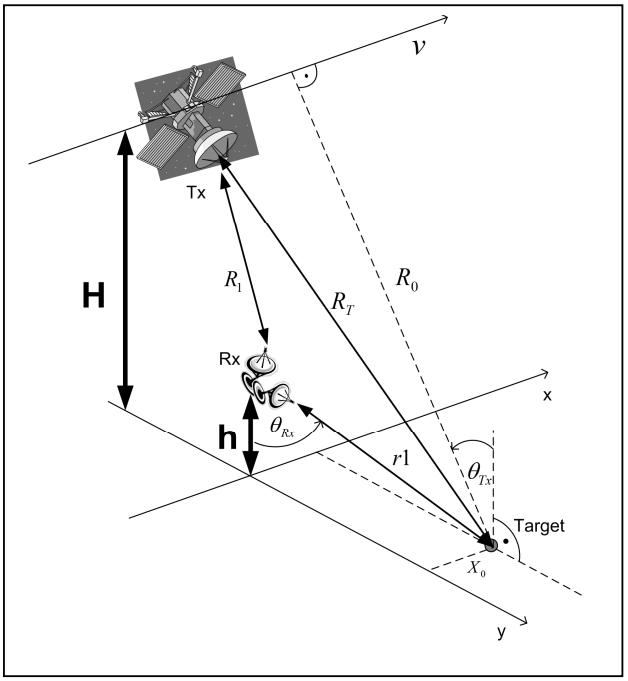

Figure 1. Simplified bistatic SAR geometry

The range resolution in passive SAR strongly depends on the bistatic geometry presented in Fig. 1 and is given by the following formula [3], [4]:

$$\delta_r = \frac{c}{B \cdot (\sin\theta_{Tx} + \sin\theta_{Rx})}, \quad (1)$$

where θ_{Tx} is the incidence angle of the transmitted signal pointing to the target, θ_{Rx} is the incidence angle of the received signal pointing to the target, B is the transmitted signal bandwidth and $c \approx 3 \cdot 10^8$ m/s is the speed of light.

The cross-range resolution for a passive SAR image is given by the following equation [3], [4]:

978-1-4577-1837-3/12/$26.00 ©2012 IEEE

$$\delta_a = \frac{\lambda}{2}\sqrt{\frac{4\cdot R_0^2}{(v\cdot T)^2}+1}\,, \tag{2}$$

where λ is the transmitted signal wavelength, R_0 is the minimum distance between the satellite and the illuminated target (see Fig. 1) and T is the integration time (time of the target illumination).

For the ground stationary receiver using the satellite transmitter as an illuminator, the following assumption is usually fulfilled:

$$\frac{4\cdot R_o^2}{(v\cdot T)^2} >> 1\,. \tag{3}$$

Then the cross-range resolution given by (2) can be approximated by the following simplified formula:

$$\delta_a = \frac{\lambda\cdot R_o}{v\cdot T}\,, \tag{4}$$

The approximation (4) is true for the assumption that $R_0 \approx R_1$. This condition is fulfilled for most ground based bistatic receivers using a spaceborne transmitter as an illuminator. For such an assumption the phase difference between the transmitter and the receiver is given by the following formula:

$$\varphi(t) \approx \frac{2\pi\cdot 1}{\lambda} + 2\pi\frac{X_0^2 + 2vtX_0}{2\lambda R_0}\,, \tag{5}$$

From equation (5) it is easy to notice that the signal received from the target located at distance X_0 in the cross-range direction is shifted in frequency by:

$$f_d = \frac{v\cdot X_0}{\lambda\cdot R_o}\,, \tag{6}$$

The frequency resolution is inversely proportional to the illumination time *T* and it is connected with the cross-range resolution by:

$$\Delta f_d = \frac{1}{T} = \frac{v\cdot\delta_a}{\lambda\cdot R_o}\,, \tag{7}$$

From equation (7) the approximation for the cross-range resolution δ_a presented by formula (4) can also be derived. Approximation (4) proposed by the authors can be successfully used for the cross-range resolution calculation for the passive SAR system using spaceborne pulsed radar as an illuminator. For example, the Envisat-1 satellite is equipped with a C-band radar ($\lambda \approx 0.0563$m) flying at the velocity *v* equals ca. 7460m/s on the average platform altitude H=790 km. Making the simplified assumption that $R_0 \approx R_1$ and the illuminated time T equals 1 second, the error of the cross-range resolution approximation given by (4) is smaller than 0.0011%.

For active SAR systems the highest possible cross-range resolution to obtain equals $L_a/2$, where L_a is the radar antenna length in the along-track direction. The antenna beamwidth in the cross-range direction can be calculated using the following formula:

$$\theta_a = \frac{\lambda}{L_a}\,, \tag{8}$$

Based on the active SAR radar geometry, the distance which the satellite passes during the target illumination time (T) can be approximated for the narrow beam radar antennas by the following formula:

$$s = vT \approx \theta_a\cdot R_0 = \frac{\lambda\cdot R_0}{L_a}\,, \tag{9}$$

Substituting $\lambda\cdot R_0/T = vL_a$ from (9) to the equation (4) gives the maximum cross-range resolution possible to achieve for passive SAR radar, which can be expressed by the following formula:

$$\delta_a = L_a\,, \tag{10}$$

The results seem to be very promising and it means that the cross-range resolution for passive SAR radar is half the quality of the well-known active SAR system.

III. Passive SAR Processing

The first step in passive SAR processing is a range compression, which can be done by correlating the reflected signal with the direct signal (in the case whereby the transmitted signal parameters are not well known), or by using matched filtering on data collected by the measurement channel (here all the parameters of the transmitted signal have to be known to be able to design the matched filter properly). The second stage is the phase and range migration correction. In next step the direct signal is removed from the reflected signal. This operation can be done using CLEAN processing [11]. The third step is a cross-range compression using FFT processing in slow time direction. This last stage involves the correction of the bistatic geometry to display the SAR image in the Cartesian domain.

IV. RESULTS

In this section the results of the passive SAR processing are presented. The simulation was done using the Raw Radar Simulator developed at the Warsaw University of Technology. In the simulated scenario it has been assumed that the illuminator of opportunity is the SAR radar mounted on the Envisat-1 satellite. The main simulation parameters are as follows: Tx velocity $v =$ 7459.98m/s, Tx altitude $H =$ 790km, Tx antenna incidence angle γ=45°, Tx signal bandwidth B =16MHz, Tx carrier frequency $f_c =$ 5.3310044GHz, Tx Pulse Repetition Frequency $PRF =$ 1686.0674Hz, Tx antenna size: 10m x 1.3m, Rx sampling frequency $f_s =$ 32MHz, integration time $T =$ 1.1862 seconds (2000 pulses) . The distance between the Rx and the center of the scene equals 1000m. The simulation was carried out using the simplified geometry presented in Fig. 1. For the algorithms tests the simplified scene consisting of 14 dominant scattering points was chosen (see Fig. 2).

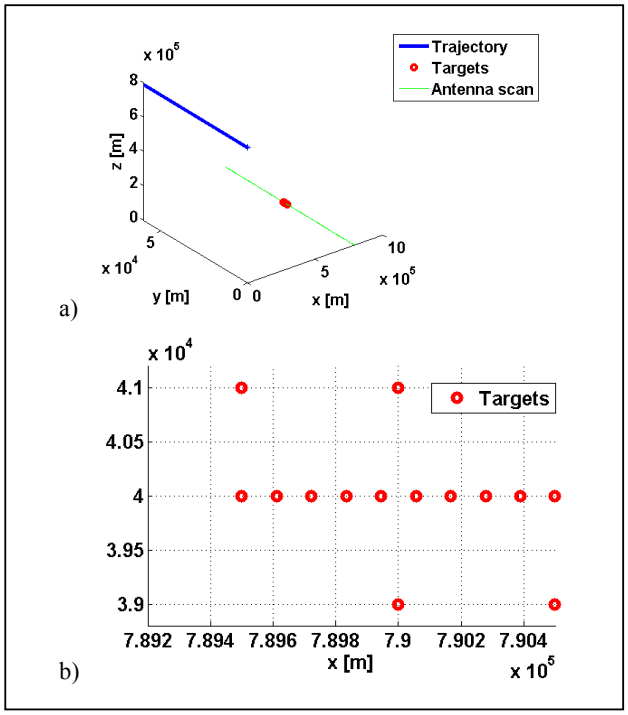

Figure 2. Simulated scene: a) simulated geometry, b) simulated ground targets

The SAR image of the scene under analysis obtained using a monostatic configuration with the active radar mounted on the Envisat-1 satellite has been shown in Fig. 3. The man-made targets can be easy recognized in the simulation results.

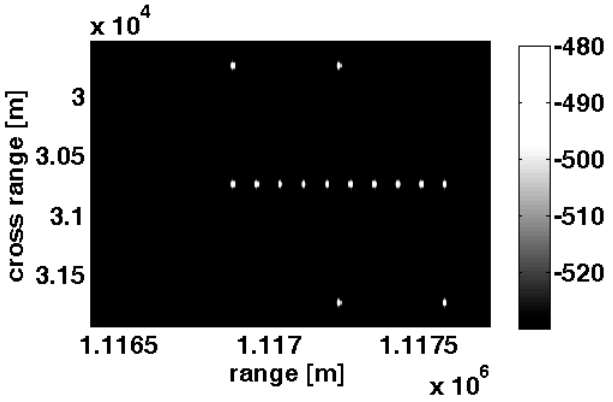

Figure 3. SAR image obtained using the active radar mounted on the Envisat-1 satellite.

In the next step the passive SAR processing for data collected by the receiver has been applied. The results of the first step of passive SAR imaging (range compression) are presented in Fig. 4. In the results presented the direct signal is visible for the first range cell. Fig. 5 represents the data after additional phase and migration correction and the direct signal removal using CLEAN processing. The strong direct signal has been successfully removed from the first range cell.

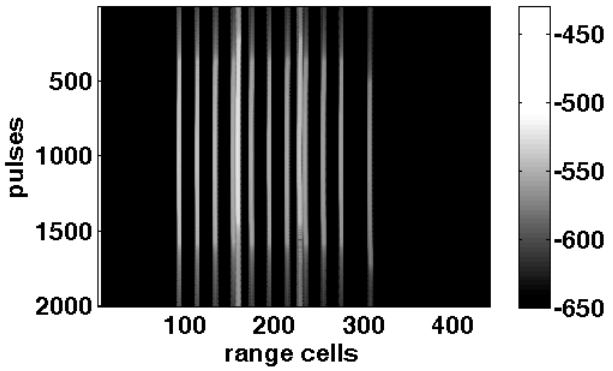

Figure 4. Raw data after range compression.

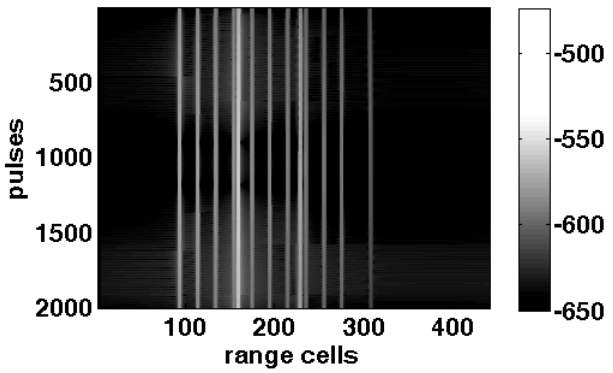

Figure 5. Raw data after range compression, phase and migration correction and CLEAN processing

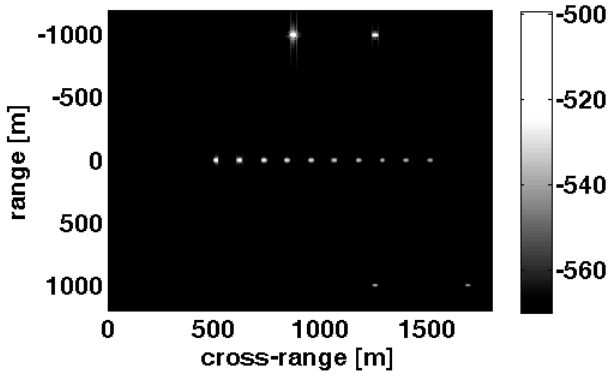

Figure 6. Passive SAR image without bistatic geometry correction

The result of the passive SAR image after cross-range compression has been shown in Fig. 6. In the result presented (see Fig. 6) the geometrical distortion of the man-made targets localization is visible. The distortion is caused by the bistatic geometry of the passive SAR scenario. The final image after the geometry conversion to the Cartesian domain is shown in Fig. 7. In comparison, the cross-range resolution of the image obtained is about twice of the result obtained in the monostatic geometry presented in Fig. 3, which confirms the theoretical analysis presented in the previous section of this paper.

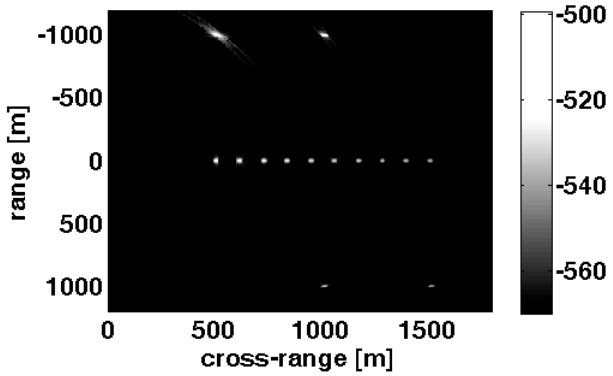

Figure 7. Passive SAR image after bistatic geometry correction

The results presented in this section successfully verify the feasibility of the passive SAR algorithms developed. The processing presented in the paper consists of few stages. It should be noted that each algorithm step has its own specified contribution to the creation of the final SAR image. To obtain the theoretical resolution given by equation (10) with the best quality of the SAR image, no stage of the processing chain presented can be omitted. As an example the SAR image obtained without the CLEAN processing is presented in Fig. 8. The direct signal is very strong and is visible in the result.

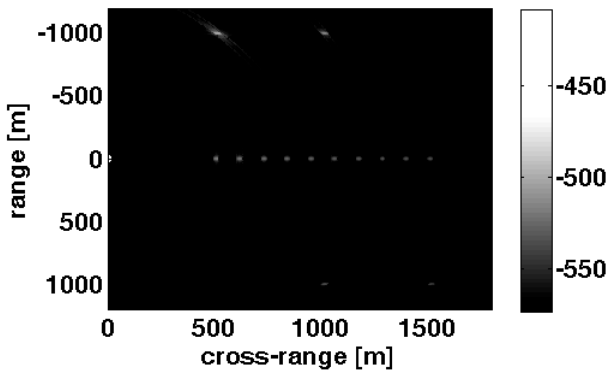

Figure 8. Passive SAR image after bistatic geometry correction without CLEAN processing

I. CONCLUSIONS

The results presented in the paper show that it is possible to obtain synthetic aperture images using a stationary receiver and a moving, non-cooperative transmitter mounted to an airborne or spaceborne platform. The range resolution of passive SAR is similar (usually slightly better) than classical monostatic SAR, while the cross-range resolution is of half the quality, since only the transmitter is moving and the receiver is stationary. The signal processing of passive SAR is simpler and has lower computational complexity than active SAR.

ACKNOWLEDGMENT

This work was supported by the European Union within the framework of the European Social Fund through the Warsaw University of Technology Development Programme.

REFERENCES

[1] N. J. Willis, Bistatic Radar, 2nd ed. SciTech Publishing Inc, 2005.

[2] N. J. Willis and H. D. Griffiths, Advances in bistatic radar. SciTech Publishing, 2007, p. 89.

[3] S. Reuter, F. Behner, H. Nies a, O. Loffeld a, D. Matthes, J. Schiller, "Development and Experiments of a Passive SAR Receiver System in a Bistatic Spaceborne/Stationary Configuration", in Proc. of IGARSS 2010, 25-30 July 2010, Honolulu, USA, pp. 118-121.

[4] G. Krieger, H. Fiedler, D. Hounam, A. Moreira, "Analysis of System Concepts for B- and Multi-Static SAR Missions", in Proc. of. IGARSS 2003, 21-25 July 2003, vol. 2, pp. 770-772.

[5] J. Sanz-Marcos, P. Lopez-Dekker, J. J. Mallorqui, A. Aguasca,P. Prats, "SABRINA: A SAR Bistatic Receiver for Interferometric Applications", in IEEE Geoscience and Remote Sensing Letters, Vol. 4, Issue 2, Arpil 2007, pp.307-311.

[6] J. Sanz-Marcos, J. J. Mallorqui, A. Aguasca, P. Prats, "First ENVISAT and ERS-2 Parasitic Bistatic Fixed Receiver SAR images processed with the Subaperture Range-Doppler Algorithm", in Proc. of IGARSS 2007, 31 July – 4 August 2006, pp. 1840-1843.

[7] S. Duque, P. Lopez-Dekker, J. J. Mallorqui, C. Lopez Martinez, "A Bistatic SAR Interferometric Simulator for Fixed Receiver Configurations," in Proc. of IGARSS 2007, 23-28 July 2007, pp. 2130-2133.

[8] W. Rui, L. Feng, Z. Tao, "Bistatic SAR Experiment, Processing and Results in Spaceborne/Stationary Configuration", in Proc. of 2011 IEEE CIE International Conference on Radar, October 24-27, 2011 Chengdu, China, Vol. I, pp. 393 – 397.

[9] P. Samczynski, K. Kulpa, M. Malanowski, P. Krysik, L. Maslikowski, "Trial results on passive SAR using Envisat-1 as illuminator of opportunity," – the paper has been accepted to be published in Proc. on EuSAR 2012 – 9th European Conference on Synthetic Aperture Radar, April 23-26, 2012, Nurnberg, Germany, in press.

[10] K. Kulpa, P. Samczynski, M. Malanowski, W. Gwarek, B. Salski, G. Tanski, "SAR Raw Radar Simulator combining optical geometry and full-wave electromagnetic approaches" – the paper has been accepted to be published in Proc. on EuSAR 2012 – 9th European Conference on Synthetic Aperture Radar, April 23-26, 2012, Nurnberg, Germany, in press.

[11] K.Kulpa: The CLEAN Type Algorithms for Radar Signal Processing, MRRS - 2008 Microwaves, Radar and Remote Sensing Symposium; 2008. pp. 152-157.